Multifunctionally wearable monitoring with gelatin hydrogel electronics of liquid metals

*Ximin Yuan[a,b], Pengcheng Wu[c], Qing Gao[c,g], Jie Xu[*a,b], Bin Guo[a,b], Yong He[*c,d,e,f]*

[a] *Key Laboratory of Micro-Systems and Micro-Structures Manufacturing Ministry of Education, Harbin Institute of Technology, Harbin 150080, China*

[b] *National Innovation Center for Advanced Medical Devices，Shenzhen, 457001, China*

[c] *State Key Laboratory of Fluid Power and Mechatronic Systems, School of Mechanical Engineering, Zhejiang University, Hangzhou 310027, China*

[d] *Key Laboratory of 3D Printing Process and Equipment of Zhejiang Province, College of Mechanical Engineering, Zhejiang University, Hangzhou 310027, China*

[e] *Cancer Center, Zhejiang University, Hangzhou, Zhejiang 310058 China*

[f] *Key Laboratory of Materials Processing and Mold, Zhengzhou University, Zhengzhou, 450002, China*

[g] *Engineering for Life Group (EFL), Suzhou, 215000, China*

[*] *Correspondence to: Yong He, e-mail: yongqin@zju.edu.cn;*

Jie Xu, e-mail: xjhit@hit.edu.cn

Supplementary Text

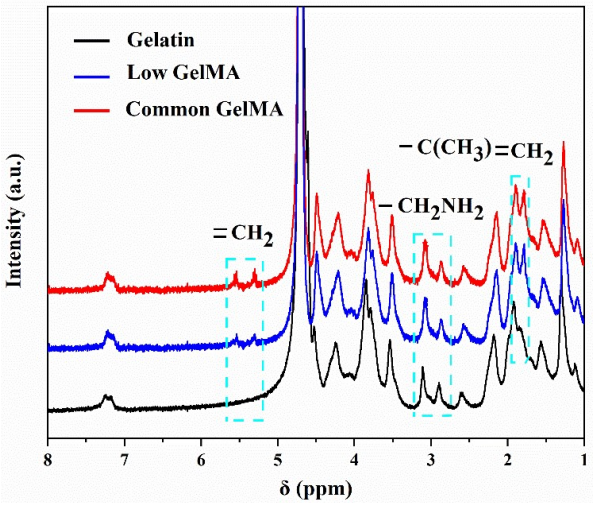

Fig. S1 NMR for gelatin and hydrogels with different replacement rates.

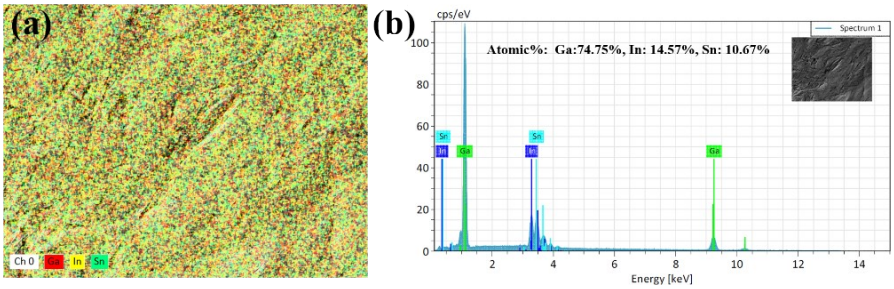

Fig. S2 EDS mapping of LMs (a) and the content of elements (b).

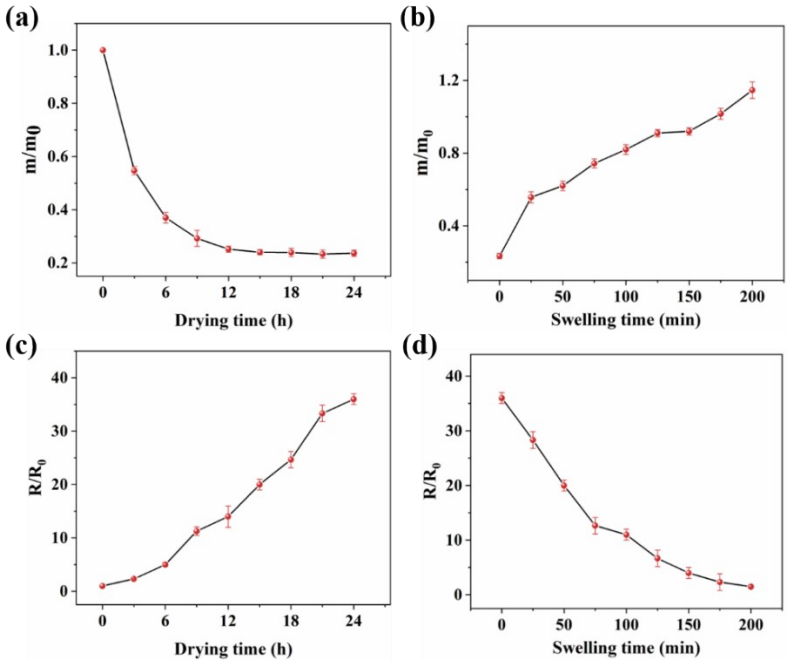

Fig. S3 The properties of LMGE as a function of time. Quality changes with the increase of drying time (a) and swelling time (b). Resistance changes with the increase of drying time (c) and swelling time (d).

According to the figures, we can independently adjust its performance (quality, resistance) according to actual needs to adapt to various applications. More importantly, LMGE can even return to its original state after being exposed to the air for 24 h, indicating its excellent reversible recovery

performance.

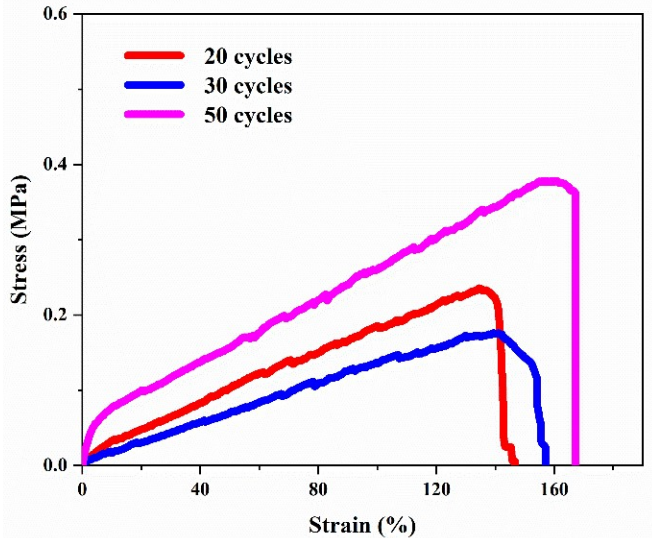

Fig. S4 Stress-Strain curves of LMGE after different numbers of drying-swelling cycles.

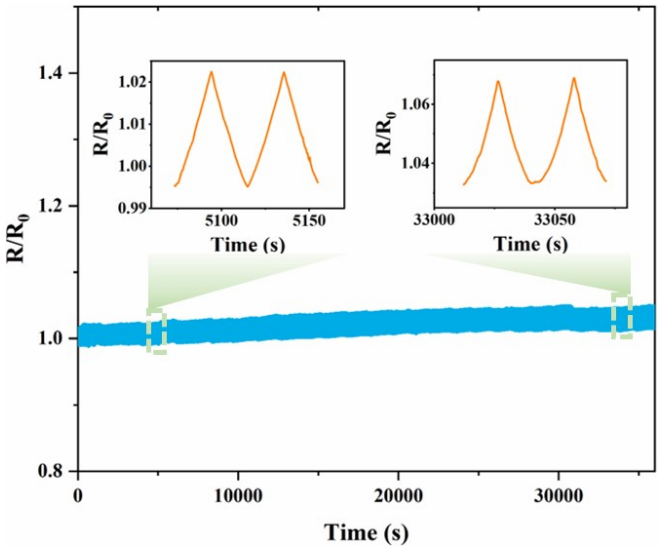

Fig. S5 Resistance changes of the LMGE after enduring different mechanical cycles.

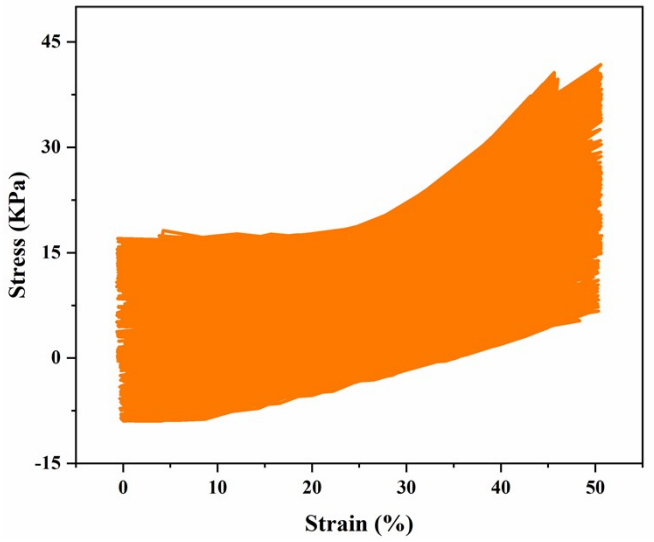

Fig. S6 Stress-strain curve of hydrogels after 1000 cycles.

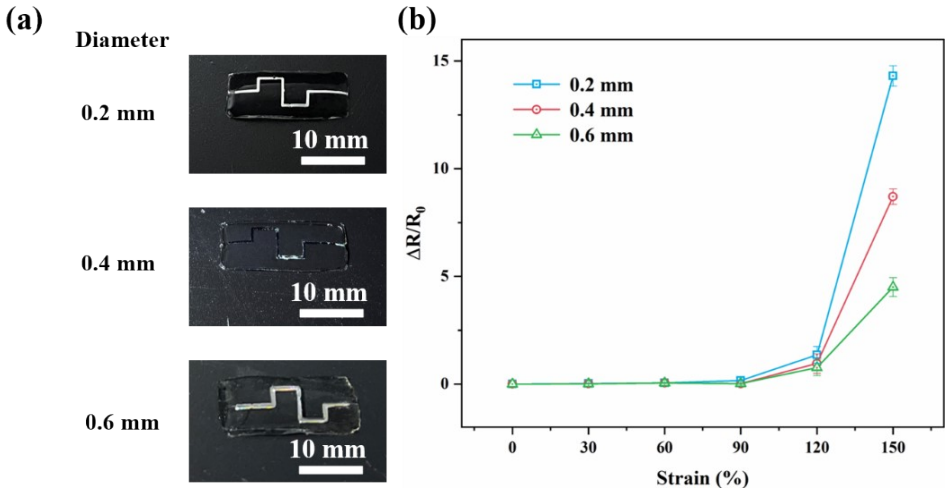

Fig. S7 Strain sensitivity of LMGE. (a) Optical images of LMGE with different diameters. (b) Strain sensing curves of LMGE with different diameters.

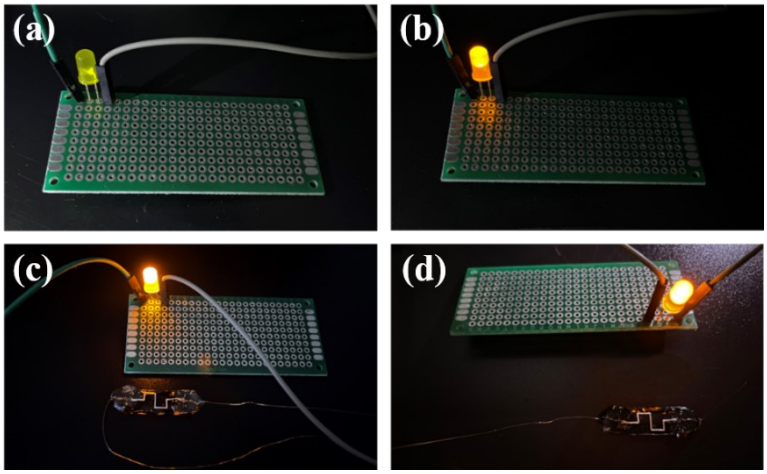

Fig. S8 LED display based on LMGE. (a) Disconnection. (b) Connection without LMGE. Connection with LMGE (c) front and (d) behind.

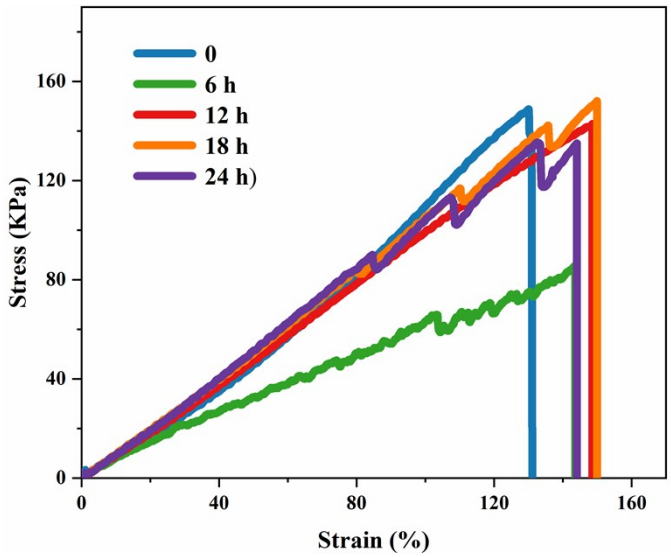

Fig. S9 Mechanical properties of LMGE covered with vaseline.

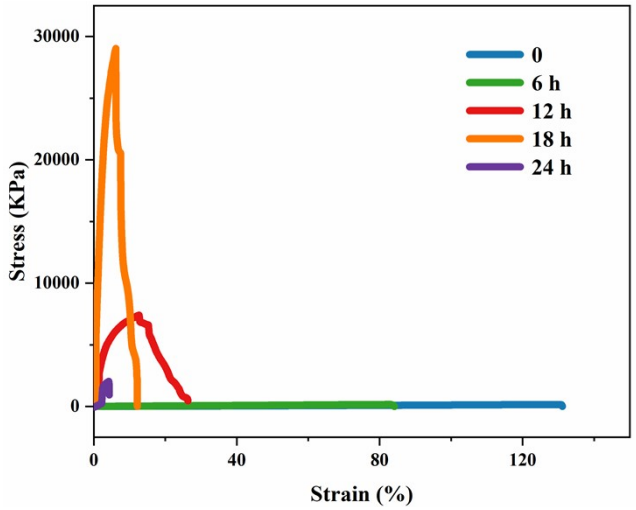

Fig. S10 Mechanical properties of LMGE uncovered with vaseline.

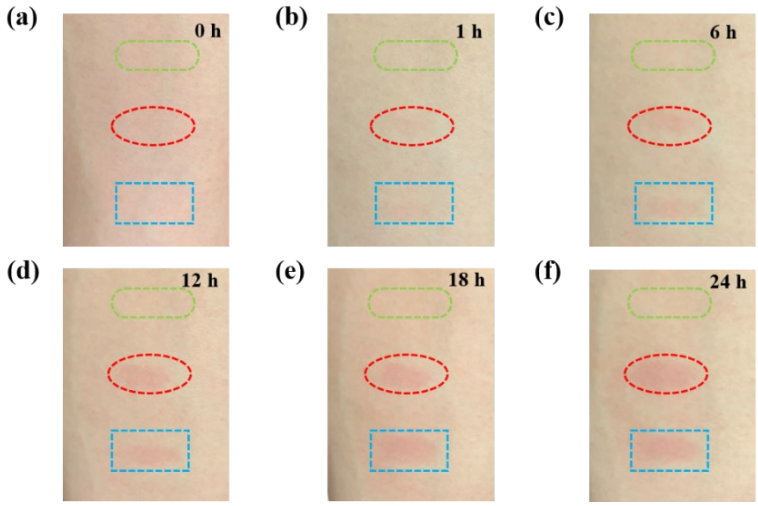

Fig. S11 Optical images showing the skin irritation results of different materials were exposed to the air for different time on the arm of the volunteer: (a) 0 h, (b) 1 h, (c) 6 h, (d) 12h, (e) 18 h, and (f) 24 h.

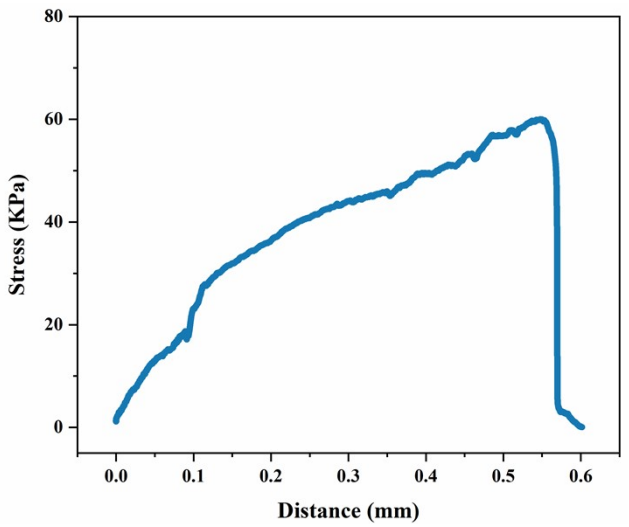

Fig. S12 Adhesion properties of hydrogels.

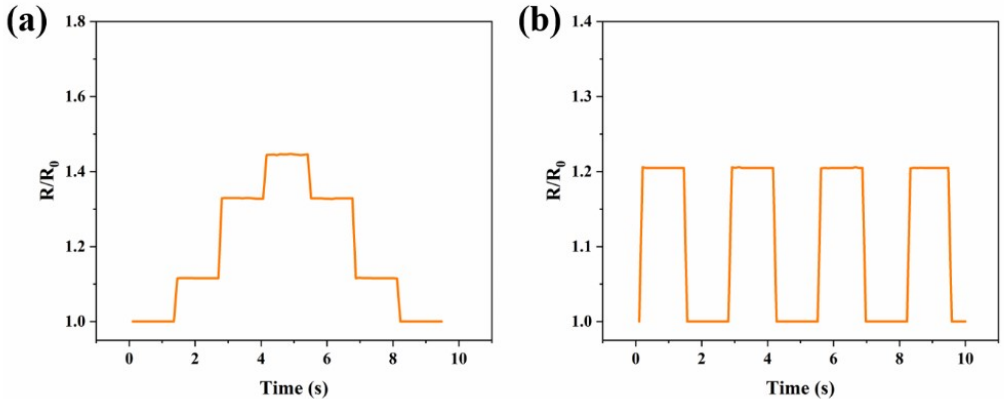

Fig. S13 Sensing performances of LMGE. (a) Current response to finger bending underwater for 24 h. (b). Current response to muscle contraction underwater for 24 h.

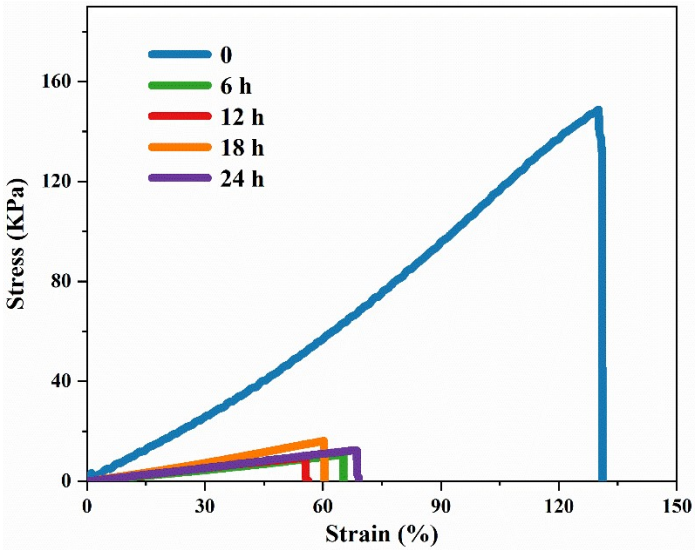

Fig. S14 Mechanical properties of LMGE after being immersed in water.

Fig. S15 Schematic diagram of monitoring scene.

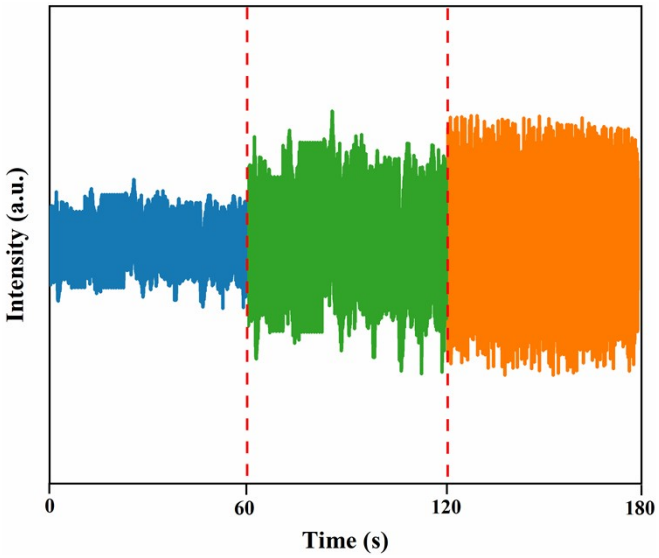

Fig. S16 Movement monitoring of LMGE.

Table S1. Comparison of different types of liquid-metal-based flexible and stretchable conductors.

Materials	Ref	Reusability	Permeability	Cycles	Monitoring capability
This study	**---**	**50**	**24 h**	**1000**	**Behaviors underwater, ECG, Sweat, Lactic acid, and Glucose**
EGaIn embedded in PAM/SA stretchable matrix	[12]	---	---	100	Behaviors
EGaIn-SBS fibre mat	[38]	---	7 days	---	ECG, Sweat
EGaIn/PVDF-HFP-TFE/MEK sheath-core microfiber	[39]	---	---	6	Behaviors

EGaIn/PDES conductive elastomer	[1]	---	---	500	Behaviors
EGaIn BMA	[40]	---	---	1000	Behaviors
Combines EBL for EGaIn thin-film	[41]	---	---	1000	Behaviors